Published May, 1992

Kernel Distributions in Main Spikes of Salt-Stressed Wheat: A Probabilistic Modeling Approach

Scott M. Lesch,* Catherine M. Grieve, Eugene V. Maas, and Leland E. Francois

ABSTRACT

Grain development in wheat (*Triticum aestivum* L.) is a complex process that responds to interactions among primary genotypic factors and the environment. This study was conducted to determine the effects of salinity stress on kernel occurrence and kernel mass distributions within the main spike. Mexican semidwarf wheat cultivars Yecora Rojo and Anza were grown in sand tanks in the greenhouse with saline and nonsaline nutrient solutions. At harvest, each spikelet position and grain position was identified and the weight of every kernel was determined. Hierarchical multiple linear regression models were derived and fit to the kernel mass patterns. In a similar manner, logistic regression models were derived and fit to the kernel occurrence patterns. Kernel mass was shown to be highly dependent on spikelet location long the spike, kernel position within the spikelet, and salinity stress. Results from the logistic regression models confirm that these same factors affect kernel occurrence. Both types of statistical analysis are advantageous, since the changes in kernel occurrence and kernel mass distributions due to each of the above factors can be easily detected and studied.

GRAIN DEVELOPMENT in wheat is a complex process that responds to interactions among many primary genotypic factors and the environment. Two important yield components, the number and mass of individual kernels, may be reduced by adverse conditions through effects on floret development and fertilization, as well as on the size and partitioning of the assimilate pool. Interactions among florets at the time of anthesis and competition between the developing kernels for photosynthates influence the number and size of the kernels that are ultimately formed. Patterns of kernel set and growth in wheat spikes have been studied by removal of competing sink sites and/or by reduction of carbohydrate supplies through defoliation and shading (e.g., Rawson and Evans, 1970; Bremner and Rawson, 1978; Pinthus and Millet,1978; Fischer and HilleRisLambers, 1978; Simmons et al., 1982; McMaster et al., 1987). Evans et al. (1972) suggested that the mechanisms involved in inhibition of kernel setting in the more distal florets and spikelets are more likely to be controlled by hormones than by competition for assimilates. Conversely, kernel development is determined by the availability of assimilates, the growth potential of the kernel and the resistance within the phloem to the movement of assimilates to the kernel (Bremner and Rawson, 1978).

Proper analysis of yield component parameters is critical for the correct interpretation and understanding of the anatomical factors involved. Analysis of these yield parameters is complicated by the physical geometry of the spike; the potential occurrence and final mass of a kernel will be influenced by both the position of the spikelet along the spike and the position of the kernel within the spikelet. A further complication arises because of the stochastic nature of the spike development process. Not all spikes under the same environmental conditions will produce the same number of spikelets, and different spikelets within the same spike can exhibit quite different kernel set and kernel mass patterns.

In this paper, kernel occurrence and kernel mass distributions in mature spikes of two Mexican hard red spring wheat cultivars (Yecora Rojo and Anza) are determined. Distribution patterns and interactions among the kernels in the nonsaline control spikes are compared with salt-stressed spikes. To facilitate these comparisons, a series of empirically based, statistical models are developed and fit to the yield component data. Through the use of such models, formal tests concerning changes in the distribution patterns caused by salinity stress can be carried out.

The development of the models and the test results concerning salinity-induced changes in kernel occurrence and kernel mass distribution patterns are presented. Additionally, we discuss the motivation behind the model parameterization, as well as an anatomical interpretation of the parameter estimates and test results.

MATERIALS AND METHODS

Plant Culture

Yecora Rojo and Anza wheat were grown in six sand tanks in the greenhouse in Riverside, CA, during January through May 1989. Details of the growth conditions are given in a companion paper (Grieve et al., 1992). Three tanks of nonsaline control plants were irrigated with a modified Hoagland's nutrient solution that had an osmotic potential (ψ_s) of -0.05 MPa and an electrical conductivity (EC_{iw}) of 2.0 dS m^{-1}. In the second set of three tanks, plants were salinized with nutrient solution that contained NaCl and $CaCl_2$ (2:1 molar basis). The ψ_s of this solution was -0.65 MPa; EC_{iw} = 14.3 dS m^{-1}.

Approximately 10 plants of each cultivar were randomly selected from each tank. Mainstem leaves were identified as they developed and were tagged with distinctively colored wire rings. Plants were harvested at maturity; main spikes were dissected and examined in detail. Each developed kernel was identified by both its spikelet position and grain position wihtin the spikelet. Spikelets were numbered acropetally, with spikelet position No. 1 being defined as the first visible node of the rachis. Within each spikelet, the basal floret (and the kernel therein) was designated as grain position 1, the second floret was designed as position 2, the third 3, etc. The recorded data consisted of whether or not a kernel occurred (developed) within each spikelet and grain position, and the weight of each developed kernel.

Since <1% of all the developed kernels occurred at or beyond Grain Position 4, we limit our investigation of ker-

U.S. Salinity Lab., USDA-ARS, 4500 Glenwood Dr., Riverside, CA 92501. Contribution from the U.S. Salinity Lab. Received 17 Dec. 1990. *Corresponding author.

Published in Crop Sci. 32:704–712 (1992).

Abbreviations: EC_{iw}, electrical conductivity of irrigation water; H_o, null hypothesis; iid, independently and identically; KMDP, kernel mass distribution potential; LDP, logistic difference probability; ψ_s, osmotic potential.

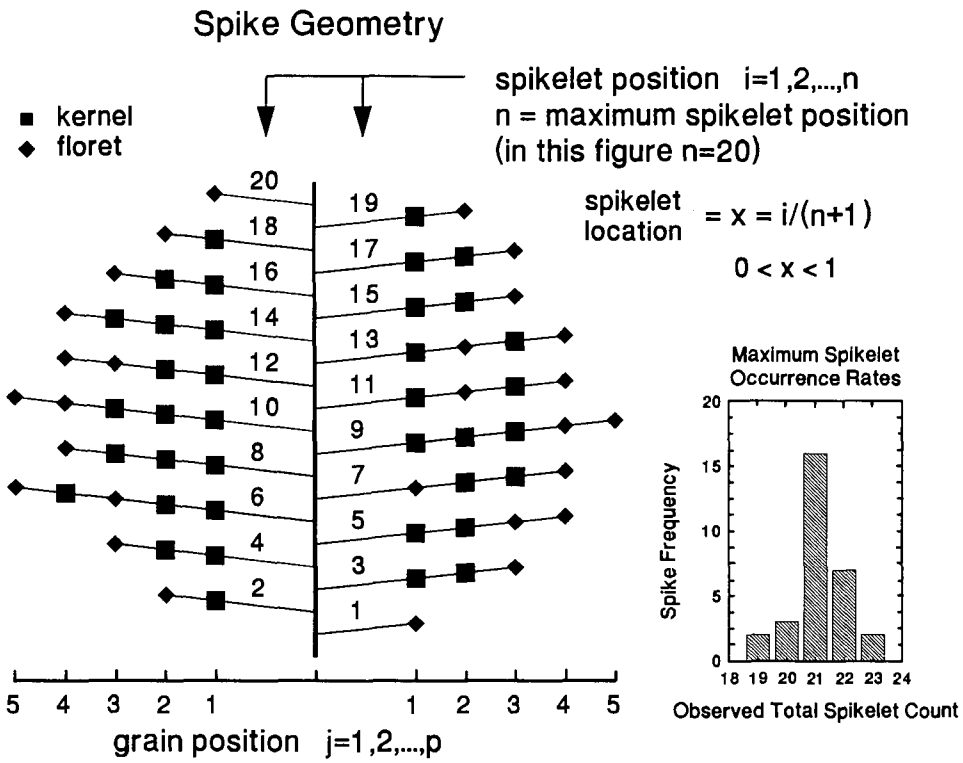

Fig. 1. Geometric representation of a spike, showing how spikelet positions can be scaled into spikelet locations. The total number of spikelets produced on the spike was considered a stochastic nuisance parameter, and was removed through the scaling procedure before comparing spikes with different spikelet counts.

nel mass and kernel occurrence data to the first three grain positions.

Spikelet Position Scaling

Statistical analyses of mainstem components based on the position of the individual kernels along the spike are complicated by the fact that, even within a given treatment, not all main spikes have the same number of spikelets. Therefore, a scaling procedure was used to facilitate the comparison of both mass and occurrence data from all the tagged plants in each treatment. Each spikelet position number was divided by 1.0 plus the total number of spikelets for that spike. Every spikelet position number was thereby converted to a spikelet location value contained within the (0,1) interval. This scaling procedure allowed for simultaneous comparison of all the yield data within a given treatment.

This scaling approach is illustrated in Fig. 1. The example spike in this diagram has a total of 20 spikelets and five potential grain positions. These spikelet positions can be converted to 20 spikelet locations by dividing each spikelet position number by 21. After such a scaling, the mass of the kernels within each grain position could be plotted (along the 0,1 spikelet location axis) and directly compared with the kernel mass data from another spike having a different number of spikelets. The histogram to the right of the example spike in Fig. 1 shows the frequency count of total number occurring spikelets per spike for Yecora Rojo in the control treatment. Note that if we had limited our analysis to only those spikes with 21 spikelets (the most common spikelet occurrence rate), we would have had to discard almost one-half of the total available data from this treatment.

Statistical Methodology and Model Parameterization

As previously implied, any statistical model used to describe either the kernel mass or occurrence data should account for both spikelet location and grain position effects. However, differences between individual spikes within a given treatment can also be quite pronounced, and should be accounted for when possible. This is especially true when modeling the kernel mass data, since specific kernel mass features can vary considerably from spike to spike.

Figures 2a and 2b highlight two important artifacts that consistently appeared in the data. In Fig. 2a, the observed kernel mass patterns within the basal grain position have been plotted for three spikes from the Yecora Rojo control treatment. Note that the relationship between kernel mass and spikelet location tends to be fairly consistent from spike to spike; i.e., the mass of the kernels in each spike tends to follow the same type of curved pattern across the spikelet locations. However, these patterns also appear to be shifted up or down the kernel mass axis. This shifting occurs because different spikes will tend to produce kernels of different mass, even under similar environmental conditions. In this paper we refer to such a change in the kernel mass distributions as a change in the spike's kernel mass distribution potential, and we develop models that can account for these KMDP differences.

In Fig. 2b, the individual kernel weights within Grain Positions 1 and 2 have been plotted for these same three spikes. Note that the correlation between the mass of these neighboring kernels is quite high. This type of correlation structure can be exploited during the modeling stage by developing hierarchical equations that relate the mass of an

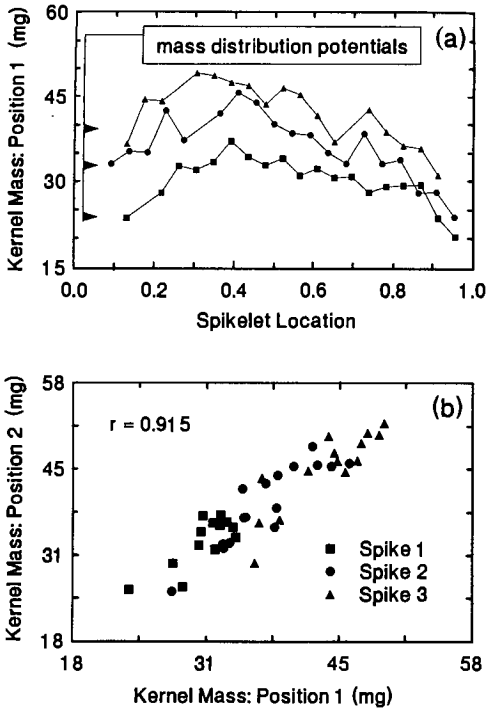

Fig. 2. (a) Example of kernel mass patterns for three Yecora Rojo control spikes exhibiting different kernel mass distribution potentials within the basal grain position, and (b) Correlation plot of the observed kernel masses occurring in the first two grain positions for the three spikes illustrated in Fig. 2a.

individual kernel to the mass of the kernel within the previous position, in addition to the spikelet location and grain position parameters. Not only will this improve the model's accuracy, it will also considerably improve our ability to correctly assess the effects of the spikelet location and grain position factors. Adjusting for the position-to-position correlation structure will help account for the differences in kernel mass between spikes, and thus separate these effects from spikelet location and/or grain position effects.

Given the above considerations, grain position specific equations can be formulated using second-order hierarchical polynomial equations, interrelated through the use of correlation and indicator parameters. For a given wheat variety and salinity stress level,

$y_{x,j,k}$ = the expected mass of a kernel occurring in the xth spikelet location and jth grain position of the kth spike,

where $x = i/(n_k + 1)$, $i = 1,2,\ldots,n_k$ (the unscaled spikelet position number), $j = 1,2,3$, and $k = 1,2,\ldots,N$. (For notational convenience, we will drop the spikelet-location subscript x during the remainder of this paper.) The kernel mass in the first grain position is defined as:

$$y_{1k} = B01_k + B11[x] + B21[x^2] + \epsilon_1 \quad [1.0]$$
$$= u_{1k} + \epsilon_1$$

where $\epsilon_1 \sim$ iid $N(0,\sigma_1^2)$, $E(y_{1k}|k) = u_{1k}$ is the expected mass of a kernel within the kth spike, and $E(y_{1k}) = u_1$ represents the expectation averaged across all spikes. B represents a regression coefficient. Brackets are used instead of subscripts, for legibility. The kernel mass within the second grain position is defined as:

$$y_{2k} = B02 + B12[x] + B22[x^2] + C2[y_1 - u_{1\cdot}] + I2[z] + \epsilon_2 \quad [2.0]$$

where x is defined as before, $\epsilon_2 \sim$ iid $N(0,\sigma_2^2)$, and z represents an indicator variable where $z = 0$ if y_{1k} exists, or $z = 1$ if no kernel occurs at y_{1k} and we replace y_{1k} with $\hat{u}_{1k}$ (estimated from 1.0). C represents a regression coefficient. The expected mass of the y_{2k} kernel within the kth spike, given the observed weight of the y_{1k} kernel, is:

$$E(y_{2k}\,|\,y_{1k}k) = B02 + B12[x] + B22[x^2] + C2[y_{1k} - u_{1\cdot}] \quad [2.1]$$
$$= u_{2k}\,|\,y_{1k}$$

The expected y_{2k} kernel mass averaged across all k spikes can then be defined to be $E(y_{2k}) = u_2$, assuming all y_{1k} kernels exist. When the y_{1k} kernel does not exist, the expected mass of the y_{2k} kernel within the kth spike becomes:

$$E(y_{2k}|k) = B02 + B12[x] + B22[x^2] + C2[u_{1k} - u_{1\cdot}] + I2 \quad [2.2]$$

The model describing kernel mass within the third grain position is:

$$y_{3k} = B03 + B13[x] + B23[x^2] + C3[y_{2k} - u_2] + I3[z] + \epsilon_3 \quad [3.0]$$

where $\epsilon_3 \sim$ iid $N(0,\sigma_3^2)$, and z again represents an indicator variable where $z = 0$ if y_{2k} exists, or $z = 1$ if no kernel occurs at y_{1k} and we set $y_{2k} = \hat{u}_{2k}|y_{1k}$ (given y_{1k} exists). I represents a regression coefficient. Since the parameterization of Eq. [3.0] is identical to Eq. [2.0], expected kernel weights can be found in the same manner as shown in Eq [2.1] and [2.2].

Each of the models defined above relates the expected kernel mass to three factors: the spikelet location, grain position, and individual spike attributes. In Eq. [1.0], the expected kernel mass distributions are assumed to have common $B11$ and $B21$ parameters within a given salinity stress level and variety; i.e., the curvilinear relationship between kernel mass and spikelet location is constant across the spikes. By allowing for individual intercept estimates, however, one can also account for potential differences in kernel mass distributions between spikes. In Eq. [2.0] and [3.0], the relationship between the kernel mass distributions and the spikelet location is again specified to be constant across the spikes, while individual spike characteristics are accounted for through the $C2$ and $C3$ correlation parameters. By exploiting both the correlation structure between neighboring kernels and the more general spikelet location and grain position dependencies, these models can effectively account for the major competing factors affecting kernel mass production. Furthermore, indicator variables are included in Eq. [2.0] and [3.0], to ascertain the effects on a kernel's mass when the kernel in the previous position fails to develop.

An important benefit derived from using these models is the ability to formally study changes in kernel mass incurred from changes in salinity stress levels. This can be done by using a general F-testing approach, as outlined in Weisberg (1985), by nesting the above equations across stress levels and then combining and/or eliminating some of the parameters. When comparing the kernel mass data within the second or third grain position across treatments, tests for changes in the correlation structures between neighboring kernels can also be carried out. In this manner, each factor that is affecting the expected kernel mass can be tested across stress levels, independently of other factors. The full and restricted model parameterization for each grain position is given in the Appendix.

Statistical models that describe the kernel occurrence distributions can be developed from logistic regression equations in the following manner. For a given wheat variety and salinity stress level, define $z_{x,j,k}$ as:

$z_{x,j,k}$ = 1 if a kernel occurs (develops) in the xth spikelet location and jth grain position of the kth spike, and
$z_{x,j,k}$ = 0 otherwise.

Next, separate the $z_{x,j,k}$ data points into nonoverlapping subsets based on their spikelet location values, where each subset represents a specific spikelet location interval contained within the (0,1) spikelet location range. Within each interval, compute the mean kernel occurrence frequency and the mean spikelet location value associated with this frequency by averaging across the $z_{x,j,k}$ data. Let $p_{q,j}$ represent these kernel occurrence frequencies and m_q represent the corresponding mean spikelet location values within the qth interval. The following logistic regression model(s) can then be fit to this data:

$$\ln[p_{q,j}/(1 - p_{q,j})] = B0_j + B1_j[m_q] + B2_j[m_q^2] + \ldots + Bt_j[m_q^t] \quad [4.0]$$

where the superscript t represents the highest order polynomial term that can be fit to the data, such that the Bt parameter estimate is found to be statistically significant.

The logistic models defined above relate the long-run, average kernel occurrence rate for a wheat plant under a specific stress level to two factors: the spikelet location and grain position. Individual spike characteristics are no longer accounted for, since the data points are based on treatment averages.

The advantage of working with averaged data is that goodness-of-fit statistics based on m-asymptotic distributional results will be usable during the model testing stages. Thus, changes in the kernel occurrence distributions across different stress levels can again be assessed with tests of homogeneity (e.g., by comparing the difference between the cumulative squared deviance residuals, from the full and reduced models, to an appropriate chi-square distribution). Note that a significant change in the sums of the deviance residuals indicates only that differences between the fitted logistic equations exist; graphical methods for determining where these differences are occurring along the spikelet location axis will be presented in the discussion section.

For a more detailed discussion on logistic regression model building and testing, the reader is referred to Hosmer and Lemeshow (1989).

RESULTS AND DISCUSSION

Kernel Mass Equations: Model Fitting and Testing

The data set consisted of 4960 developed kernels from 188 spikes; Table 1 gives total kernel counts by wheat type, treatment level, and grain position. Sixty-three kernels were deleted during the model-building analysis; 58 of these kernels were only partially developed, and 5 were abnormally large. Additionally, 99.8% of all the developed kernels occurred within the first three grain positions.

The kernel mass equation parameter estimates and summary statistics, found with the SAS (1985) GLM procedure, are given in Table 2. Aside from the indicator variables, t-test statistics revealed that all parameter estimates except one were significant well below an $\alpha = 0.01$ level. Furthermore, six of the eight indicator parameters were significant at or below an $\alpha = 0.02$ level, and a seventh indicator parameter was significant at about an $\alpha = 0.05$ level. These equations tend to explain the kernel mass data well, with 9 out of the 12 fitted models explaining between 78 and 88% of the observed variability. The mean-square error estimates were usually ≈10.0 mg, suggesting that the mass of an individual kernel could generally be predicted to within ≈6.3 mg of its ture value 95% of the time.

Table 1. Number of developed kernels at each grain position for Yecora Rojo and Anza wheat main spikes.†

Grain Position	Yecora Rojo Osmotic potential, MPa		Anza Osmotic potential, MPa	
	−0.05	−0.65	−0.05	−0.65
	no.			
1	507 (7)‡	438 (6)	560 (6)	515 (6)
2	418 (3)	418 (8)	497 (4)	487 (4)
3	221 (4)	237 (5)	281 (7)	318 (3)

† The full data set consisted of 4960 kernels from 118 spikes; however, a total of 63 kernels were abnormally developed and therefore deleted from the analysis.
‡ Number of kernels deleted from the analysis are given in parentheses.

Plots of predicted vs. observed kernel mass data within the first three grain positions are shown in Fig. 3 for a typical Yecora Rojo spike grown under the -0.05 MPa control treatment. In the first grain position, note that the predicted kernel weights follow a smooth quadratic curve, as dictated by Eq. [1.0]. Fitting a unique intercept estimate allowed this curve to adjust for this spike's particular kernel mass distribution potential (the KMDP estimate for this spike was 23.87 mg). However, the model for this first grain position cannot respond to individual kernel weights that deviate too far from the general curve, such as the first kernel mass (identified in Fig. 3 by the letter A). The second and third grain-position models can respond to individual kernel mass deviations through both the correlation and indicator parameters. Note that the observed and predicted kernel mass identified by the letter B in the Position-2 plot are nearly identical; this agreement occurs because knowledge of the unusually low mass of the preceding kernel (A) is used in the model. In a similar manner, the high observed and predicted kernel mass identified by the letter C in the Position-3 plot occurs in part because no kernel developed in the previous position. Hence, the indicator parameter in Eq. [3.0] added 3.07 mg to the grain mass estimate.

The tests statistics concerning changes in kernel mass distributions across treatment levels are given in Table 3. All the general F-tests concerning spikelet location parameters reveal highly significant salinity influences. There is also some evidence within the Yecora Rojo cultivar that estimates of adjacent kernel correlations decreased at the higher salinity level (Table 2). This pattern was not evident in the Anza cultivar.

Kernel Occurrence Equations: Model Fitting and Testing

Before the kernel occurrence models could be developed, it was necessary to average the $z_{x,j,k}$ data. This was done by separating each treatment data set into 12 nonoverlapping subsets based on the spikelet location values. Each subset covered exactly 8% of the total spikelet location axis; the subset bounds were defined to be (0.02,0.10), (0.10,0.18), (0.18,0.26), . . ., (0.90,0.98). (Spikelet location values never fell below 0.02 or above 0.98.) The total number of spi-

Table 2. Parameter estimates: Kernel mass equations for two wheat cultivars. (All parameter estimates are significant at the 0.01 level, unless otherwise noted.)

Grain position	Parameter	Yecora Rojo		Anza	
		Osmotic potential (MPa)		Osmotic potential (MPa)	
		−0.05	−0.65	−0.05	−0.65
1	$E(B01_k)$	30.26‡	37.25‡	19.69‡	30.51‡
	$B11$	50.82	58.64	68.31	63.30
	$B21$	−58.56	−61.23	−66.27	−64.45
2	$B02$	29.30	30.70	18.71	26.42
	$B12$	67.36	101.6	88.34	95.66
	$B22$	−79.88	−108.5	−91.65	−101.7
	$C2$	0.872	0.773	0.830	0.748
	$D2$	1.895†	1.395*	1.484§	1.694†
3	$B03$	18.60	1.160§	9.921	7.743
	$B13$	75.69	190.1	98.47	139.6
	$B23$	−99.29	−217.1	−111.1	−152.1
	$C3$	0.809	0.631	0.875	0.924
	$D3$	3.070†	8.193	3.435	4.680
1	R^2	0.867	0.779	0.825	0.802
	MSE (mg)	11.14	7.74	5.96	5.55
2	R^2	0.872	0.842	0.783	0.878
	MSE (mg)	9.42	10.65	9.59	6.36
3	R^2	0.839	0.652	0.641	0.651
	MSE (mg)	8.94	17.00	11.71	11.41

*,† Significant at the 0.05 and 0.02 levels, respectively.
‡ All individual intercept estimates are significant at the 0.01 level.
§ Not significantly different from 0.

kelets falling within each of these subsets represents the maximum potential kernel occurrence counts (if kernels had occurred in every one of the spikelets within a subset, then this subset would have had a 100% kernel occurrence rate). The total number of developed kernels within each grain position in each subset were then divided by the maximum potential kernel occurrence count to produce the kernel occurrence rates (the $p_{q,j}$ frequencies). The mean spikelet location values associated with these subsets (the m_q values) were defined to be the arithmetic average of all the individual spikelet location values falling within each subset.

The decision to split the $z_{z,j,k}$ data into exactly 12 subsets was not made arbitrarily. It was decided a priori that each of the m_q estimates should be based on ≈50 potential kernel occurrence counts. Partitioning the data into 12 subsets generally achieved this goal.

The logistic regression models were fit to these data by using the SAS CATMOD procedure (SAS, 1985); the resulting maximum-likelihood parameter estimates for each model are shown in Table 4. All the parameter estimates were significant through the second degree well below the $\alpha = 0.01$ level, indicating that a very strong relationship existed between the average kernel occurrence rate and spikelet location.

The cumulative deviance values (and corresponding χ^2 probabilities) are given at the bottom of Table 4. These goodness-of-fit statistics suggest that the logistic regression models fitted to the Anza kernel occurrence rates were sufficient in explaining all of the observed occurrence rate variability. This was not the case for three of the six logistic regression models to fit to the Yecora Rojo data.

The predicted vs. observed kernel occurrence rates for the Anza data at -0.05 MPa are shown in Fig. 4 for the first three grain positions. In these plots, pre-

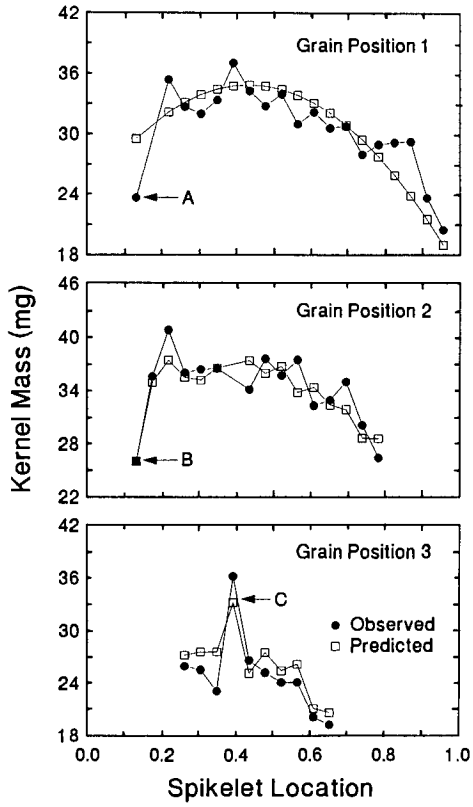

Fig. 3. Predicted versus observed kernel masses for grain positions 1, 2, and 3 at each spikelet location in a Yecora Rojo control spike. "A": unusually low kernel mass in position 1; "B": the correct prediction of low kernel mass in position 2, based on the knowledge of the low kernel mass in position 1; "C": a correct upward adjustment in the prediction of the kernel mass in position 3, based on the knowledge of no kernel development in position 2.

Table 3. General *F*-tests: Kernel mass equations for wheat.

Grain position	Full model RSS†	Full model df	Reduced model RSS	Reduced model df	Hypothesis‡	*F*-value	Probability
				Yecora Rojo			
1	8307.89	868	8629.88	870	(*B*111,*B*211) = (*B*112,*B*212)	16.23	0.0001
2	8176.90	815	27787.8	818	(*B*021,*B*121,*B*221) = (*B*022,*B*122,*B*222)	651.5	0.0001
2	8176.90	815	8229.70	816	(*C*21) = (*C*22)	5.26	0.0221
3	5755.98	439	13333.0	442	(*B*031,*B*131,*B*231) = (*B*032,*B*132,*B*232)	192.6	0.0001
3	5755.98	439	5856.37	440	(*C*31) = (*C*32)	7.66	0.0059
				Anza			
1	5783.01	1003	5897.01	1005	(*B*111,*B*211) = (*B*112,*B*212)	9.89	0.0001
2	7720.45	966	23942.2	969	(*B*021,*B*121,*B*221) = (*B*022,*B*122,*B*222)	676.6	0.0001
2	7720.45	966	7739.92	967	(*C*21) = (*C*22)	2.44	0.1186
3	6687.10	579	13904.5	582	(*B*031,*B*131,*B*231) = (*B*032,*B*132,*B*232)	208.3	0.0001
3	6687.10	579	6691.20	580	(*C*31) = (*C*32)	0.35	0.5543

† Residual sum of squares.
‡ Equations given in Appendix.

dicted rates are represented by the smooth curves. The observed average rates within each grain position appear to be well described by the fitted equations for this cultivar and treatment level.

The general χ^2 test statistics, computed from the difference of the deviance scores, are shown in Table 5. All of the χ^2 statistics were significant well below the $\alpha = 0.01$ level, suggesting that the observed kernel occurrence distributions within both cultivars were influenced by the increased salinity.

Salinity-Induced Changes in the Kernel Mass Distributions

As indicated in Table 3, all of the general *F*-tests concerning spikelet location parameters revealed that significant changes in these estimates were occurring across the treatments. Therefore, understanding how these changes affect the estimated kernel mass becomes important.

Changes in observed kernel mass *averages* across treatments were discussed in detail in Grieve et al. (1992). Here we concentrate instead on how and where changes occur in the estimated maximum kernel mass. The fitted response equations were used to determine for each grain position the spikelet location yielding the maximum kernel mass and the estimated kernel mass for that location. In Table 6, the predicted kernel mass at the maximum kernel mass location is given for each grain position within both cultivars and treatment levels. Increases in the estimated maximum kernel mass ranged between 22 and 29%; all increases were statistically significant. Additionally, the largest kernel mass always occurred in Grain Position 2, the next largest in Position 1, and the smallest in Position 3. These results are similar to those found by Grieve et al. (1992) concerning changes in the average kernel mass across treatment levels.

The *F*-tests shown in Table 3 also suggest that a change in the kernel-to-kernel correlation structure may have occurred within the Yecora Rojo cultivar across treatment levels. However, the variability associated

Table 4. Parameter estimates: Kernel occurrence equations for two wheat cultivars. All parameter estimates are significant at the 0.01 level, unless otherwise noted.

Grain position	Parameter	Yecora Rojo osmotic potential (MPa) −0.05	Yecora Rojo osmotic potential (MPa) −0.65	Anza osmotic potential (MPa) −0.05	Anza osmotic potential (MPa) −0.65
1	*B*01	−4.388	−10.03	−2.732	−7.492
	*B*11	45.56	112.9	23.57	68.64
	*B*21	−76.19	−324.4	−19.11	−114.9
	*B*31	35.28	379.6	NS	55.26
	*B*41	NS‡	−157.0†	NS	NS
2	*B*02	−4.450	−6.067	−3.725	−6.410
	*B*12	34.66	47.01	27.77	50.54
	*B*22	−36.22	−65.15	−25.65	−73.16
	*B*32	NS	25.01*	NS	29.06
3	*B*03	−7.527	−15.21	−4.760	−8.850
	*B*13	43.20	78.16	26.92	49.98
	*B*23	−50.58	−79.95	−28.89	−51.26
1	Deviance	8.96	14.30	11.64	10.06
	(Probability)	(0.346)	(0.046)	(0.235)	(0.261)
2	Deviance	23.21	17.03	13.56	3.74
	(Probability)	(0.006)	(0.030)	(0.139)	(0.879)
3	Deviance	10.88	4.98	14.72	7.26
	(Probability	(0.284)	(0.836)	(0.099)	(0.610)

*,† Significant at the 0.05 and 0.02 levels, respectively.
‡ Parameter was not statistically significant, and hence was not included during the final model estimation process.

with the Yecora Rojo KMDP estimates decreased substantially when the −0.65 MPa stress level was applied, from 51.64 mg down to 11.25 mg. This in turn implies that the range in which an individual kernel mass could occur was reduced by half. Such a reduction is bound to lower the correlation estimate, since the strength of the kernel-to-kernel correlation will be directly related to the range of the kernel mass data. Therefore, it seems more likely that the application of salinity stress caused the average kernel mass between spikes to behave more uniformly, rather than changing the correlation structure within the spike itself. This conclusion is supported by the lack of any significant

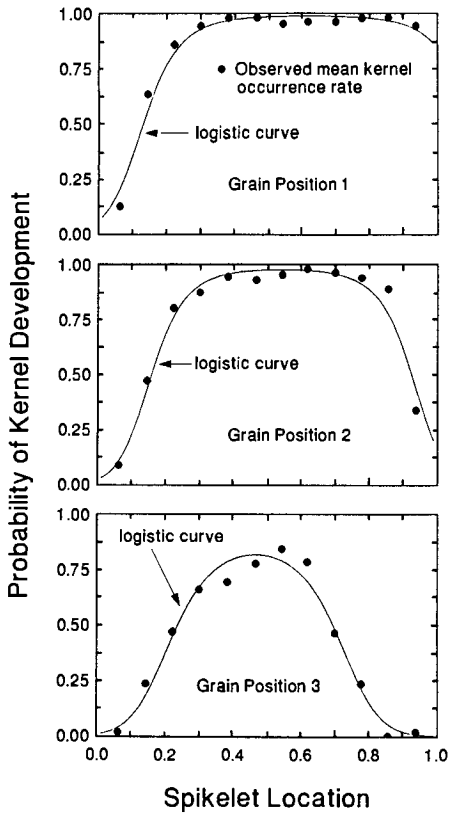

Fig. 4. Predicted versus observed mean kernel occurrence rates for grain positions 1, 2, and 3 at each spikelet location in Anza control spikes.

Table 5. General chi-squares tests: Kernel occurrence equations for two wheat cultivars.†

Grain position	Full model Deviance	df	Reduced model Deviance	df	χ^2 value	Probability
			Yecora Rojo			
1	20.40	14	48.17	19	28.03	0.0001
2	40.15	16	183.4	20	143.3	0.0001
3	15.86	18	107.6	21	91.72	0.0001
			Anza			
1	13.78	16	37.30	20	23.52	0.0001
2	15.35	16	30.75	20	15.40	0.0039
3	21.97	18	68.57	21	46.60	0.0001

† Hypothesis: The fitted logistic regression parameter estimates do not change between the −0.05 MPa and −0.65 MPa treatments.

changes in the correlation parameter estimates for Anza (where the corresponding reduction in the variability of the KMDP estimates was much less severe).

The effect on a kernel's mass when the kernel in the previous position fails to develop can be seen directly in Table 2. The estimates associated with the indicator variables imply that, in this case, the average mass of a kernel increased anywhere from 1.4 to 8.2 mg. These results indicate that the loss of a kernel within a spikelet may be partially compensated for by an increase in the mass of the adjacent kernel. Previous work (Rawson and Evans, 1970; Bremner and Rawson, 1978; Pinthus and Millet, 1978) has shown that removal of sink sites by sterilization of neighboring (adjacent) florets, particularly those in the central spikelets, leads to increased growth of the remaining kernels. This response may be the result of reduced competition for supplies of assimilates, minerals, and internal growth substances. Alternatively, this response may be due to the removal of an inhibitory effect, perhaps one of a hormonal nature.

Table 6. Estimated mass of kernel at the maximum kernel mass location for two wheat cultivars.

Grain Position	Osmotic potential (MPa) −0.05	−0.65	Increase due to salinity†
	mg		%
	Yecora Rojo		
1	41.29	51.29	24.2
2	43.50	54.48	25.2
3	33.02	42.78	29.6
	Anza		
1	37.29	46.20	23.9
2	40.00	48.92	22.3
3	31.74	39.77	25.3

† Defined as: % change = [mass (−0.65 MPa) − mass (−0.05 MPa)]/mass (−0.05 MPa).

Table 7. Average kernel occurrence rates in two wheat cultivars across treatments.

Grain Position	Yecora Rojo Osmotic Potential (MPa) −0.05	−0.65	Anza Osmotic Potential (MPa) −0.05	−0.65
	%			
1	79.97	84.72	85.89	82.93
2	65.93	80.85	76.23	78.42
3	34.86	45.84	43.10	51.21

Salinity-Induced Changes in the Kernel Occurrence Distributions

The χ^2 test statistics in Table 5 confirm that the kernel occurrence distributions were also changing across treatment levels. As shown in Table 7, raising the salinity level tended to raise the overall average kernel occurrence rate within each grain position (with the exception of the first grain position in Anza); however, to understand how these kernel occurrence rates change along the spikelet location axis, direct comparisons of the fitted logistic regressions should be made.

One way to make such a comparison would be to plot the logistic curves predicted under both treatments on the same graph and look for where they differ. A natural extension of this approach would be to subtract one curve from the other; i.e., subtract the predicted kernel occurrence rates under the −0.65 MPa treatment from the predicted rates under the −0.05 MPa treatment at every point along the spikelet location axis. The resulting curve would represent the difference between the predicted probabilities, and hence the change in the kernel occurrence rate subject to a change in the spikelet location.

These types of plots, referred to in this paper as logistic difference probability plots, are shown for each cultivar and grain position in Fig. 5. There are some striking similarities between the LDP plots. For example, within the first quarter of the spike, the kernel

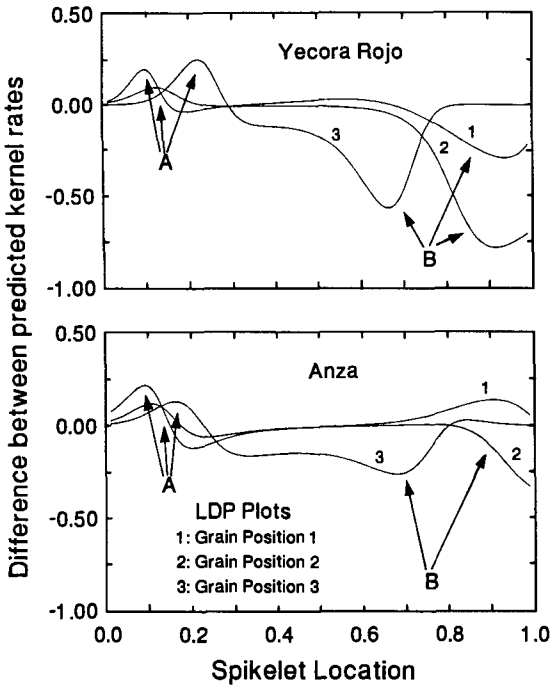

Fig. 5. Logistic difference probability plots for Yecora Rojo and Anza cultivars showing the effect of salinity on the predicted kernel occurrence rates for grain positions 1, 2, and 3 within the spikelet. The ordinate records the excess of the occurrence rate for the control over the stress treatment. Note the areas along the spike of increasing kernel occurrence rates under "A" (control conditions) and "B" (stress conditions).

occurrence rates in the control treatments tended to exceed the rates in the salinity treatments anywhere from 10 to 25%, regardless of the grain position or cultivar. These areas of increasing probabilities are identified by the letter A within Fig. 5. Five of the six LDP plots also show that a simultaneous increase in the kernel occurrence rates took place under the salinity treatment. These increases, which tended to occur more toward the terminal end of the spike, are identified by the letter B in Fig. 5.

The cumulative effect of salinity stress on kernel development seems to be a general readjustment of the kernel occurrence distributions. Under salinity stress, the kernel production potential in both cultivars seemed to have drop slightly near the spike base, but then increase more strongly up toward the spike apex. The only exception to this occurred with the first grain position in Anza, which showed a slightly higher kernel occurrence potential at both the spike base and apex.

Anatomical Interpretations

Spikelets are linked in parallel to the source of assimilates along the rachis. However, this parallel linkage does not imply that each spikelet can access the same amount of assimilates during kernel filling; rather, both the potential for kernel production and the ultimate kernel mass are strongly influenced by the position of the spikelets along the spike. This influence of spikelet position (location) is also clearly subject to individual spike characteristics and the prevailing environmental conditions during the growth of the plant.

Bremner and Rawson (1978) found a clear indication of a partial in-series linkage within the spikelets themselves. The degree of correlation between adjacent kernels found in this study seems to support such a hypothesis. The magnitude of the correlation parameter estimates within the models suggest that the mass of an individual kernel is strongly influenced by factors unique to each spikelet, in addition to spikelet location and grain position effects. These factors could again be related to the actual amount of available assimilates, which would explain the consistent increase or decrease in kernel mass occurring throughout the spikelet. It is not clear, however, what effect (if any) the environmental conditions may have on this in-series linkage.

Thornley et al. (1981) presented a model to predict kernel growth in response to changing environmental conditions that is based on spikelet anatomy and includes assumptions on pathway resistance to assimilate movements and biochemical response functions. We wish to stress that the models presented here are empirically based statistical models, which should not be interpreted as (nor can they take the place of) anatomically based models. However, proper formulation and interpretation of such statistical models can increase our understanding of the morphological processes that influence grain yield. In this manner, the maximum amount of information contained within the experimental data can be extracted and used in the formulation and/or testing of models based on anatomical assumptions.

CONCLUSION

Both kernel production and kernel mass are influenced by many factors within a spike. These factors include physical characteristics, such as the spikelet location and grain position of each kernel, as well as many complicated anatomical factors. Kernel production and mass are also influenced by environmental conditions, such as temperature, available light and nutrient supply, and salinity, among others.

The results found in this study indicate that salinity stress can have a strong effect on the final kernel occurrence and kernel mass distributions within the spikes. Furthermore, the results indicate that these mass and occurrence distributions tend to be reasonably predictable, once the physical characteristics mentioned above are accounted for.

Finally, we believe the statistical modeling approach presented here should prove useful for other types of nondestructive grain development studies, such as light or nutrient deprivation studies, temperature stress studies, etc. These types of models provide a comprehensive way to assess the effects of the treatment variable in relation to the different physical characteristics of the spike, and thereby increase our potential for understanding the underlying anatomical mechanisms inherent in the spike development process.

APPENDIX

The kernel mass model parameterization used to compute the F-values listed in Table 3 is described below.

Grain Position 1

Define k1 = 1, 2, . . ., N_1 and $k2$ = 1, 2, . . ., N_2. For kernel mass data from the −0.05 MPa level, define

w0 = 1, w1 = x, w2 = x^2, v0 = 0, v1 = 0, v2 = 0; for data from the −0.65 MPa level, define w0 = 0 w1 = 0, w2 = 0, v0 = 1, v1 = x, v2 = x^2. The full model is parameterized as:

$$[A]\quad E(y_{1[k1,k2]}) = B01_{k1}[w0] + B01_{k2}[v0] + B111[w1] + B211[w2] + B112[v1] + B212[v2]$$

The reduced model is parameterized as:

$$[B]\quad E(y_{1[k1,k2]}) = B01_{k1}[w0] + B01_{k2}[v0] + B11[x] + B21[x^2]$$

The computed F-value represents a formal test of the hypothesis

$$H_0: (B111,B211) = (B112,B212).$$

Rejection of this test implies that the spikelet location (linear and quadratic) parameter estimates are changing across the treatment levels.

Grain Position 2

For kernel mass data from the −0.05 MPa level define w0 = 1, w1 = x, w2 = x^2, v0 = 0, v1 = 0, v2 = 0, and r1 = $y_{1k} - \hat{u}_{1.}$, z1 = 0 (if the kernel in Position 1 occurs) or r1 = $\hat{u}_{1k} - \hat{u}_{1.}$, z1 = 1 (if the kernel in Position 1 does not occur), r2 = 0, and z2 = 0. For data from the −0,65 MPa level define w0 =0, w1 = 0, w2 = 0, v0 = 1, v1 = x, v2 = x^2, r1 = 0, z1 = 0, r2 = $y_{1k} - \hat{u}_{1.}$, z2 = 0 (if the kernel in Position 1 occurs) or r2 = $\hat{u}_{1k} - \hat{u}_{1.}$, z2 = 1 (if the kernel in Position 1 does not occur).

The full model is parameterized as:

$$[A]\quad E(y_{2k}) = B021[w0] + B022[v0] + B121[w1] + B122[v1] + B221[w2] + B222[v2] + C21[r1] + C22[r2] + I21[z1] + I22[z2]$$

The reduced model which is used to test for equivalent spikelet location parameter estimates across treatment levels is:

$$[B]\quad E(y_{2k}) = B02 + B12[x] + B22[x^2] + C21[r1] + C22[r2] + I21]z1] + I22[z2]$$

The formal hypothesis being tested is:

$$H_0: (B021,B121,B221) = (B022,B122,B222)$$

The reduced model which can be used to test for an equivalent correlation parameter estimate is:

$$[C]\quad E(y_{2k}) = B021[w0] + B022[v0] + B121[w1] + B122[v1] + B221[w2] + B222[v2] + C2[y_{1k} - u_{1.}] + I21[z1] + I22[z2]$$

The formal hypothesis being tested through this equation is:

$$H_0: (C21) = (C22).$$

Grain Position 3

For kernel mass data from the −0.05 MPa level define w0 = 1, w1 = x, w2 = x^2, v0 = 0, v1 = 0, v2 = 0, and r1 = $y_{2k} - \hat{u}_{2.}$, z1 = 0 (if the kernel in Position 2 occurs), or r1 = $\hat{u}_{2k}|y_{1k} - \hat{u}_{2.}$, z1 = 1 (if the kernel in Position 2 does not occur), r2 = 0, and z2 = 0. For data from the −0.65 MPa level define w0 = 0, w1 = 0, w2 = 0, v0 = 1, v1 = x, v2 = x^2, r1 = 0, z1 = 0, and r2 = $y_{2k} - \hat{u}_{2.}$, z2 = 0 (if the kernel in Position 2 occurs), or r2 = $\hat{u}_{2k}|y_{1k} - \hat{u}_{2.}$, z2 = 1 (if the kernel in Positon 2 does not occur). The full model is parameterized as:

$$[A]\quad E(y_{3k}) = B031[w0] + B032[v0] + B131[w1] + B132[v1] + B231[w2] + B232[v2] + C31[r1] + C32[r2] + I31[z1] + I32[z2]$$

The reduced model which is used to test for equivalent spikelet-location parameter estimates across treatment levels is:

$$[B]\quad E(y_{3k}) = B03 + B13[x] + B23[x^2] + C31[r1] + C32[r2] + I31[z1] + I32[z2]$$

The formal hypothesis being tested is:

$$H_0: (B031,B131,B231) = (B032,B132,B232)$$

The reduced model which can be used to test for an equivalent correlation parameter estimate is:

$$[C]\quad E(y_{3k}) = B031[w0] + B032[v0] + B131[w1] + B132[v1] + B231[w2] + B232[v2] + C3[y_{2k} - u_{2.}] + I31[z1] + I32[z2]$$

The formal hypothesis being tested through this equation is:

$$H_0: (C31) = (C32).$$

REFERENCES

Bremner, P.M., and H.M. Rawson. 1978. The weights of individual grains of wheat ear in relation to their growth potential, the supply of assimilate and interaction between grains. Aust. J. Plant Physiol. 5:61–72.

Evans, L.T., J. Bingham, and M.A. Roskams. 1972. The pattern of grain set within ears of wheat. Aust. J. Biol. Sci. 25:1–8.

Fischer, R.A., and D. HilleRisLambers. 1978. Effect of environment and cultivar on source limitation to grain weight in wheat. Aust. J. Agric. Res. 29:443–458.

Grieve, C.M., S.M. Lesch, L.E. Francois, and E.V. Maas. 1992. Analysis of main-stem yield components in salt-stressed wheat. Crop Sci. 32:697–703 (this issue).

Hosmer, D.W., Jr. and S. Lemeshow. 1989. *Applied Logistic Regression*. John Wiley & Sons, New York.

McMaster, G.S., J.A. Morgan, and W.O. Willis. 1987. Effects of shading on winter wheat yield, spike characteristics, and carbohydrate allocation. Crop Sci. 27:967–973.

Pinthus, M.J., and E. Millet. 1978. Interactions among number of spikelets, number of grains and grain weight in the spikes of wheat (*Triticum aestivum* L.) Ann. Bot. 42:839–848.

Rawson, H.M., and L.T. Evans. 1970. The pattern of grain growth within the ear of wheat. Aust. J. Biol. Sci. 23:753–764.

SAS Institute. 1985. The GLM and CATMOD procedures. *In* SAS User's Guide: Statistics. Version 5 ed. SAS Institute, Inc., Cary, NC.

Simmons, S.R., R.K. Crookston, and J.E. Kurle. 1982. Growth of spring wheat kernels as influenced by reduced kernel number per spike and defoliation. Crop Sci. 22:983–988.

Thornley, J.H.M., R.M. Gifford, and P.M. Bremner. 1981. The wheat spikelet—growth response to light and temperature—experiment and hypothesis. Ann. Bot. 47:713–725.

Weisberg, S. 1985. Applied linear regression. John Wiley & Sons, New York.